Solar Physics (2023) 298:103
https://doi.org/10.1007/s11207-023-02198-3

RESEARCH

Relationships Between Physical Parameters of Umbral Dots Measured for 12 Sunspot Umbras with the Goode Solar Telescope

M. Ali Calisir[1] · H. Tayfun Yazici[1] · Ali Kilcik[1] · Vasyl Yurchyshyn[2]

Received: 10 May 2023 / Accepted: 11 August 2023 / Published online: 5 September 2023

Abstract

We present a comprehensive analysis of the physical parameters and relationships of umbral dots (UDs), which assists in our understanding of the physical properties of the Sun. This study is based on a detailed analysis of UDs detected in 12 umbras belonging to 10 different sunspots using high-resolution data recorded by the Goode Solar Telescope at Big Bear Solar Observatory. We obtained the physical parameters (total intensity, diameter, eccentricity, lifetime, and dynamic velocity) of each UD and calculated correlation coefficients using linear and nonlinear approaches to reveal the relationships between these parameters. We found that: i) The diameter of UDs vary between 92.2 km and 246.5 km, the eccentricity varies between 0.02 and 0.65, the lifetimes of UDs vary from 0.75 to 120.00 min and the dynamic velocities vary from 0.01 $\mathrm{km\,s^{-1}}$ to 3.80 $\mathrm{km\,s^{-1}}$. ii) The intensity–diameter and diameter–eccentricity relationships show the highest degree of correlation, while the lowest linear correlation was obtained for the diameter–lifetime relationship and the lowest nonlinear correlation was obtained for the eccentricity–lifetime relationship. iii) In general, the nonlinear correlation coefficients are higher than the linear correlation without exception. iv) The linear and nonlinear correlation coefficients are very close to each other in the case of the diameter–eccentricity relation. v) While the average diameter, intensity, and eccentricity are related to the umbral area, the average lifetime and dynamic velocity of UDs are not dependent on the umbral area.

Keywords Sunspots · Umbra · Physical parameters · Linear–nonlinear relation

✉ A. Kilcik
alikilcik@akdeniz.edu.tr

M.A. Calisir
muhammed.calisirr@gmail.com

H.T. Yazici
htayfunyazici@gmail.com

V. Yurchyshyn
vasyl.yurchyshyn@njit.edu

[1] Department of Space Science and Technologies, Akdeniz University Faculty of Science, 07058 Antalya, Turkey

[2] Big Bear Solar Observatory, New Jersey Institute of Technology, Big Bear City, CA 92314, USA

1. Introduction

The observational instruments and methods used to investigate solar physics are rapidly advancing with the development of new technologies. With the advancing technology, sunspots and their fine structure, as well as their physical properties, are being studied in more detail. A well-developed sunspot is fundamentally composed of two main parts: the umbra, situated at the center of the spot and characterized by its pronounced darkness, and the penumbra, which surrounds the umbra and appears lighter compared to the umbra. Umbral dots (UDs) are one of the most prominent fine structures observed in the sunspot umbra. UDs are observed as small, bright patches of various sizes split in two or more fragments by thin dark lanes. UDs were first observed by Stanislas Chevalier in 1916 as bright specks within the umbra (Choudhuri, 1986). Thiessen (1950) first identified smaller-scale UDs, which were subsequently discovered by Robert Danielson in 1964 using stratoscope (a balloon-borne astronomical telescope) observations (Danielson, 1964; Thomas and Weiss, 2004).

It is known that UDs play an important role in the energy balance of the sunspot (Tritschler and Schmidt, 1997; Schüssler and Vögler, 2006; Watanabe, Kitai, and Ichimoto, 2009). Sunspots show a wide range of dynamic variations throughout their lifetimes. The umbral and penumbral regions of a sunspot are also affected by these variations (Solanki, 2003). Understanding the internal dynamics and evolution of sunspots still involves challenges with current technology. However, our developing knowledge and observation technologies about UDs are guiding factors to understanding the structure and evolution of sunspots. Attempting to relate the physical properties of UD's to the large-scale characteristics of sunspots enables the creation of realistic sunspot models. However, the underlying physical processes affecting the evolution and stability of sunspots are not well understood yet. Despite the increase in resolution of observations with advancing technology, the more accurate calculation of UD parameters and a complete understanding of the formation and underlying mechanisms of UDs still remain elusive in the literature. Thus, elucidation of the physical parameters and relationships among UDs is of great importance for understanding the physical properties of sunspots.

Over time, the progress of image-processing techniques and high-resolution analysis have improved UD detection, thus advancing our understanding of sunspots. The physical properties of UDs have been extensively studied using various techniques and datasets. Watanabe et al. (2012) used data from the CRISP instrument operating at the Swedish Solar Telescope to find that the average lifetime of UDs is approximately 18 min. Kilcik et al. (2012) analyzed data from the Goode Solar Telescope (GST) operating at the Big Bear Solar Observatory (BBSO) and reported a lower average lifetime of 8 min with variations between 2.5 and 34.5 min. Feng et al. (2015) investigated the UD lifetimes using Hinode data and found that the lifetime varies between 1 and 36 min. Hashem (2020) obtained an average lifetime of 7.4 min for UDs based on Hinode/Solar Optical Telescope (SOT) data. Recently, Kilcik et al. (2020) refined the analysis and found that the UD lifetime varies between 45 s and 65 min with an average lifetime of 7 min.

It was reported that the UD diameter ranges between 50 to 750 km (Sobotka and Hanslmeier, 2005; Riethmüller et al., 2008; Watanabe et al., 2012; Kilcik et al., 2012; Feng et al., 2015; Yadav, Louis, and Mathew, 2018a; Kilcik et al., 2020). Based on Hinode/SOT data, Feng et al. (2015) reported the UD size of 225 km, while Ji et al. (2016) analyzed data from the New Vacuum Solar Telescope (NVST) and found that the UD diameter varies between 178 and 235 km. Hashem (2020) measured the UD diameter to be $\sim$0.25 arcsec (180 km), while the analysis of 2892 UDs revealed that the diameter ranged from 107 to 276 km with a mean diameter of 207 km (Kilcik et al., 2020).

A remarkable difference exists among the UD parameters obtained by different authors using various data (e.g., Watanabe et al., 2012; Feng et al., 2015; Ji et al., 2016; Kilcik et al., 2020). These studies are generally based on analysis of one or a few sunspots and commonly utilize Hinode/SOT data. In this study we used GST data acquired with a 1.6 m clear aperture telescope. The GST has an advantage of high spatial (0.1 arcsec) and temporal (10 s) resolution, thus allowing for more precise measurements and more accurate results.

Two previous studies using GST data, were based on a single sunspot measurement, allowed, for the first time, to measure UD eccentricity (Kilcik et al., 2012) and define the dynamic velocity of UDs (Kilcik et al., 2020). Earlier, Schüssler and Vögler (2006) reported horizontally elongated UDs found in their simulations. Kilcik et al. (2012) have confirmed this simulation result and found that without exception, all observed UDs exhibited an elliptical shape. Feng et al. (2015) reported that UDs have an average eccentricity of 0.75. Kilcik et al. (2020) noted that the eccentricity of UDs has a much smaller mean value of 0.29, which was measured using Hinode/SOT data.

Different studies investigating the relationship between UD parameters have yielded varying or similar results. Bharti, Beeck, and Schüssler (2010) reported that larger UDs are brighter and have longer lifetimes. Using data from NVST, IRIS, and SDO, Deng (2019) reported that the diameter and lifetime of UDs exhibited an increasing trend along with brightness, but their velocities did not increase or showed a reverse trend. Based on Hinode/SDO data Yadav and Mathew (2018b) concluded that UD intensity and size, intensity and lifetime, and size and lifetime are positively correlated. Ji et al. (2016) reported positive correlation of UD sizes and lifetimes with brightness, while no such correlation was observed for UD velocities.

On the other hand, Kilcik et al. (2012) and Hashem (2020) did not detect any correlation between the lifetime and the mean intensity or size of UDs. Instead, the UD brightness exhibited approximately equal correlation with both diameter and dynamic velocity, while the UD diameter showed much higher correlation with eccentricity (Kilcik et al., 2020). These authors also could not find a relationship between the lifetime and dynamic velocity, as reported in other studies. It should be noted that many studies are often based on data for a single or a few sunspots observed within a short time period, or results of simulations. In the present study, we measured physical parameters (total intensity, diameter, eccentricity, lifetime, and dynamic velocity) of UDs for 12 sunspots observed with GST between 2015 and 2022, which covers a period from the maximum of Solar Cycle 24 to the maximum of Solar Cycle 25. In this study, linear and nonlinear correlation analyses were performed to reveal possible relationships between the physical parameters of UDs. To the best of our knowledge, a nonlinear correlation analysis was applied to UD parameters for the first time in this study.

The outline of the article is as follows: In Section 2, we present the data, methods used, and analysis results. In Section 3, a discussion and our conclusions are presented.

2. Data, Methods, and Analysis Results

2.1. Data Preparation

The data used in the study cover the 2015 – 2022 time interval. Ten ARs were selected from the GST archive. All ARs were located within a 30° radius from the solar disk center (see Table 1) to minimize the projection effect. Two AR sets included sunspots with multiple umbras, which were separately analyzed in the study, so that the total number of analyzed

Table 1 List of the analyzed sunspots and some of their properties.

Data set	NOAA active region number	Date	Sunspot location	Cadence [s]	Seeing quality
1	AR12384	14/07/2015	S18W19	15	good
2	AR12411	08/09/2015	N14E13	15	good
3	AR12565 (dual umbra)	14/07/2016	N04E30	15	good
4	AR12767	28/07/2020	S20W18	15	good
5	AR12770 (dual umbra)	08/08/2020	N23E11	15	fair
6	AR12776	20/10/2020	S13W17	15	fair
7	AR12902	30/11/2021	N18W03	15	good
8	AR12934	24/01/2022	S25E16	15	good
9	AR13046	06/07/2022	N18W05	20	good
10	AR13053	12/07/2022	N16W20	20	fair

umbras was 12. The data consist of photospheric images acquired using a broadband TiO filter. Note that the instrument setup remained the same and adaptive optics were utilized for all observations. The TiO spectral band is highly sensitive to temperature, making it well suited for observations of dark and cool regions, including umbra (Berdyugina, Solanki, and Frutiger, 2003; Riethmüller et al., 2008; Abramenko et al., 2010). All TiO datasets were speckle reconstructed using the Kiepenheuer-Institute Speckle Interferometry Package (Wöger and von der Lühe, 2007) and the resulting field of view (FOV) was $70 \times 70''$, with the pixel scale of $0.034''$. The cadence of the data was 15 s, except for two sunspots that were observed with a 20 s cadence. For the analysis we selected time intervals with good seeing that were stable over at least one hour of observations. Occasional images with unacceptable quality were removed from the time series (see Table 1). All images in a dataset were carefully coaligned and destretched and the residual image displacement was estimated to be less than 100 km (3 pixels). Note that the same instrument setup was employed for all observations.

The following steps were performed prior to applying an automatic UD detection algorithm. First, an image sequence was smoothed to determine the umbra–penumbra (UP) boundary using intensity thresholding (see Figures 1 and 2). The threshold was set to 0.75 of the mean intensity of the entire sunspot including the surrounding quiet Sun area immediately adjacent to the sunspot. The same threshold was applied to all datasets and we concluded that it worked quite well for our data. There is no standard approach to determining the UP boundary. Thomas and Weiss (2004) stated that the average penumbral intensity is about 75% of the quiet Sun intensity, I_{QS}, measured outside of a sunspot. Mathew et al. (2007) calculated average cumulative intensity histograms for 88 symmetrical sunspots and found that the UP intensity threshold is $0.655 I_{QS}$. Later, Valio et al. (2020) used SOHO data to find that the threshold of $0.655 I_{QS}$ corresponds to a temperature of 5196 K, and, in their data, the temperature threshold for the UP boundary was set to 5200 K. Next, high-frequency intensity fluctuations were eliminated by applying a Fast Fourier Transform (FFT) filter that removed brightness differences and errors caused by observational and atmospheric effects, following the methods used by Watanabe, Kitai, and Ichimoto (2009), Kilcik et al. (2012) and Ebadi, Abbasvand, and Pourjavadi (2017). Finally, we normalized the final umbra image by dividing it by the mean intensity of the 100×100 pixel area selected from an outside quiet region of each sunspot.

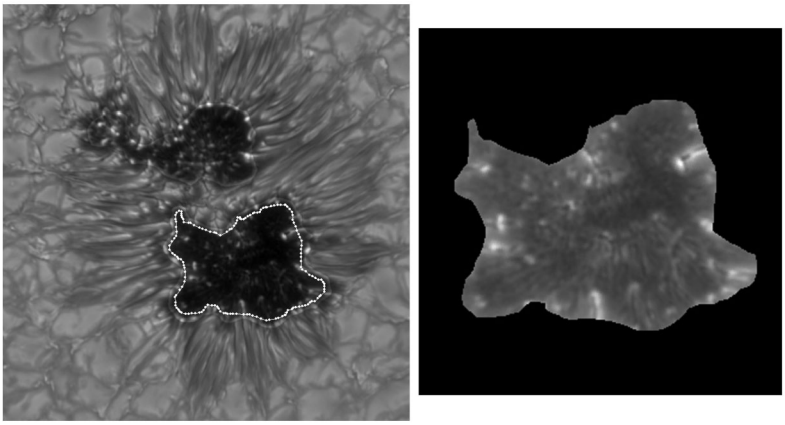

Figure 1 Selection of a large umbral core in NOAA AR 12770 (left) and the zoomed in extracted umbral core (right). The sizes of images are 711 × 711 pixels and 311 × 311 pixels, respectively.

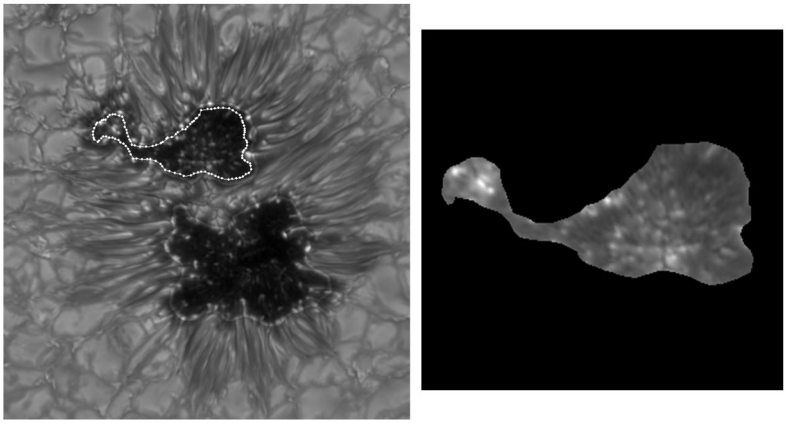

Figure 2 The same as in Figure 1 but for the small umbral core in NOAA AR 12770. The sizes of images are 711 × 711 pixels and 311 × 311 pixels, respectively.

2.2. UD Detection, Tracking, and Measurements of Their Parameters

To detect and track UDs we used the modified particle-tracking code originally written by Crocker and Hoffman (2007). The tracking criteria were chosen as follows. The largest UD diameter and separation between two UDs were set to 370 km (15 pixels) visually from the reference image, which is one of the best-quality images in the data cube. To describe the largest UD diameter we measured the largest distance between two edges of the largest UD in the reference image and a few pixel greater value used as the upper limit of the diameter. It was reported earlier that the average UD speed is about 0.34 km s^{-1}, which suggests that a UD may travel as far as 5 km within a 15 s interval, which is below the limit on the maximum distance of 124 km (5 pixels) set in the tracking routine. If a UD does not appear in three consecutive images then it reappears it is counted as a new UD and takes a new identification (ID) number.

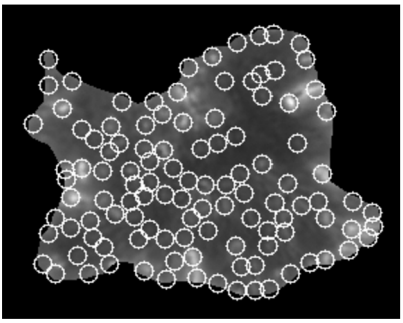

Figure 3 Detected UDs in the large umbral core of NOAA AR 12770.

We also accepted that a UD should appear at least in three consecutive images, thus eliminating short-living UDs or detection errors as much as possible. Figure 3 shows several elongated penumbral grains near the umbra–penumbra boundary that were marked as UDs due to temporal variations of the umbra. We would like to note that the number of these peripheral UDs is very low and they do not affect the final results. For each detected UD, we documented its coordinates within the image, total intensity, radius, eccentricity, and the UD ID number. The total intensity was calculated as the sum of intensities of all pixels within an UD area. The code provides the central coordinates and radius of a detected UD and thus the UD area was defined as a circle (see Figure 3). The UD radius and eccentricity are calculated directly, as suggested in the original code (Crocker and Weeks, 2021). Eccentricity is zero for circles and one for lines. Thus, if the eccentricity is not zero the UD has an elongated shape. The radius is the radius of gyration. The lifetime was calculated using data cadence and the total number of frames in which a given UD was detected. To calculate the dynamic velocities of UDs, we used the lifetime and the length of the track made by each UD. Finally, each detected UD in each data cube was tracked and we calculated mean UD parameters by averaging over the lifetime.

In Figure 4 we show the distribution of the parameters obtained for NOAA AR 12770. The dynamic velocity of UDs shows a nearly Gaussian distribution excluding very fast UDs (dynamic velocity $> 1.5\ \mathrm{km\,s^{-1}}$). We used this histogram to determine outlier events, where we accepted that very slow UDs may be due to the background noise, while very fast UDs may be due to alignment problems or misidentifications. Then, two different approaches were applied to the dynamic velocities. First, we used the box plot method also known as Interquartile Range (IQR), in which the distribution of data is evaluated based on quartile values (minimum, first quartile (Q1), median, third quartile (Q3), and maximum (see, Tukey, 1970, 1977, for more information). Here, the median is the middle value of the dataset, Q1 is the middle number between the smallest number and the median of the dataset, Q3 is the middle value between the median and the highest value of the dataset. The IQR is described as the 25th to the 75th percentile. Thus, the maximum is equal to Q3+1.5IQR and the minimum is equal to Q1-1.5IQR. These maximum and minimum values describe the upper and lower limits and any values outside those limits are accepted to be outliers (Frigge, Hoaglin, and Iglewicz, 1989; Hyndman and Fan, 1996; Rousseeuw, Ruts, and Tukey, 1999; Dekking et al., 2005). Note that the upper and lower limits are different for each parameter and also for each AR. Secondly, all events that had their lifetimes close to the length of the dataset were removed after checking the lifetime distribution of the sample. After these two approaches, on average 4.48% of all detected UDs were removed from the list and final datasets were obtained and used for the analysis.

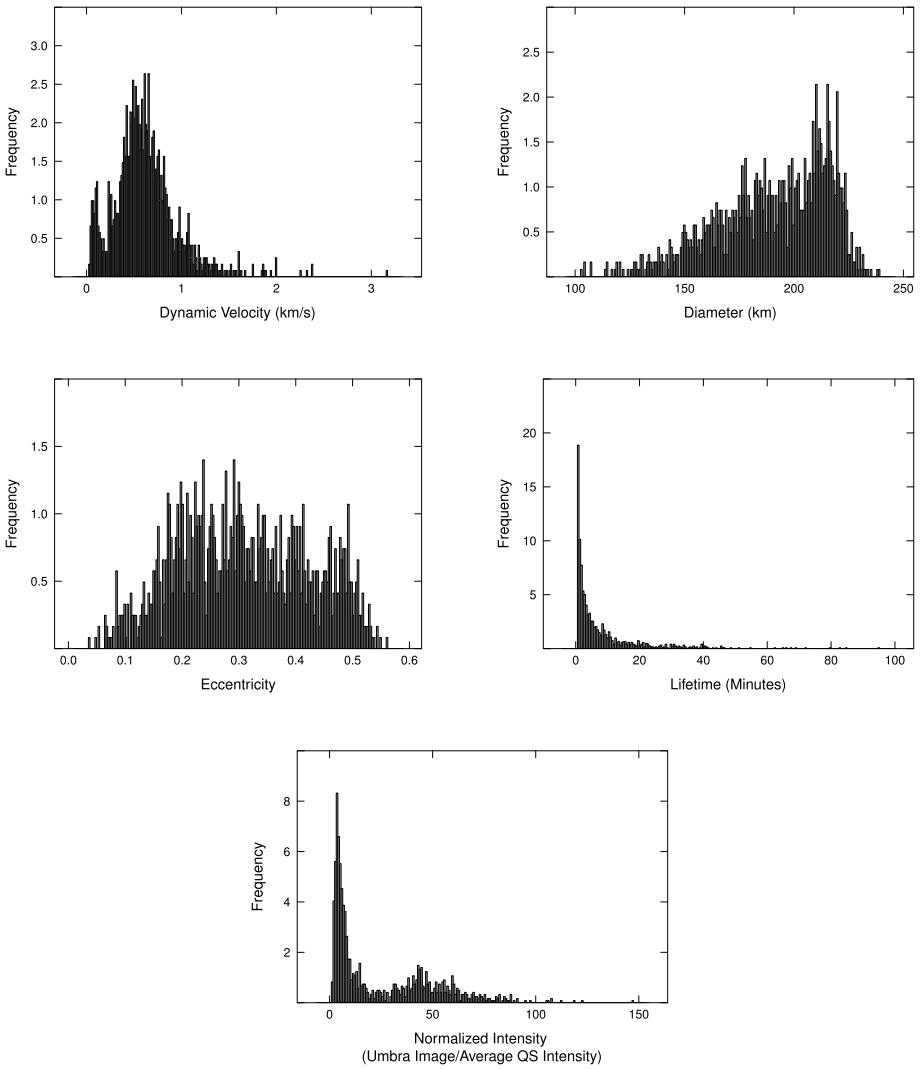

Figure 4 Histograms for the large umbral core of NOAA AR 12770.

As seen in Figure 4, the intensity distribution shows a double-hump structure and this feature is observed in all analyzed umbras without exception. The double-hump feature can also be detected in the diameter and eccentricity distributions, but it is less prominent there. Note that the lifetime behaves in a completely different way, which has a very long extended tail.

2.3. Comparison of UD Parameters

In Figure 5, we present scatter plots of various UD parameters for NOAA AR 12770. Best fits and the corresponding regression equations are also presented in these graphs. The best fit for the mean UD intensity and diameter is an exponential curve, while linear fits were

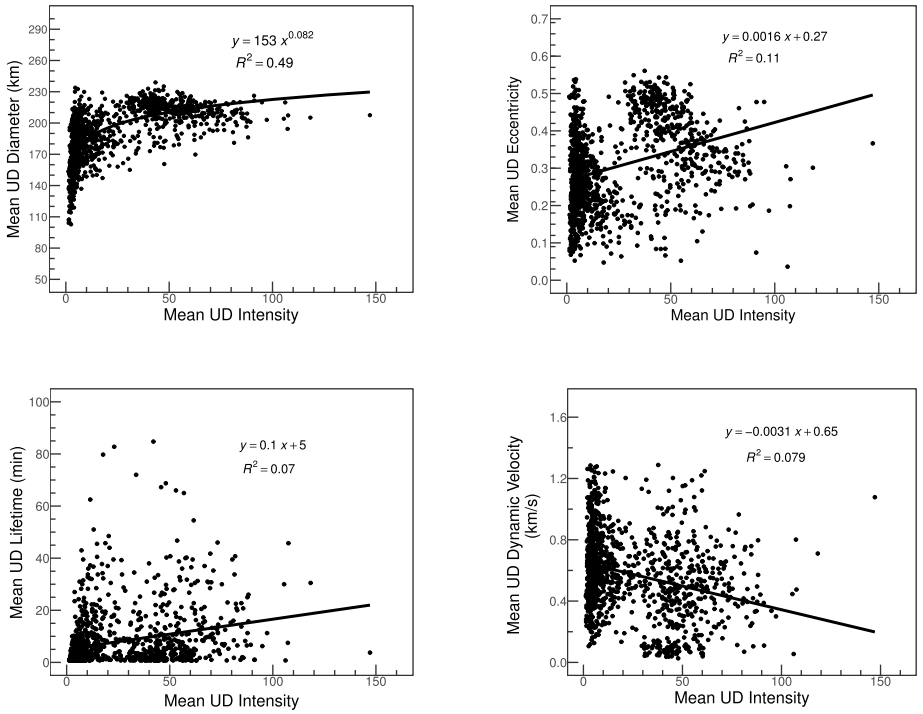

Figure 5 Relationships between selected UD parameters detected in the large umbral core of NOAA AR 12770.

chosen to fit all other pairs. To investigate the relationship between UD parameters, we performed correlation analysis using linear and nonlinear approaches. We measured correlation between all mean UD parameters. Linear correlation coefficients, r, were calculated by using the Pearson correlation function and their errors were obtained from the Fisher test statistic.

To estimate the nonlinear correlation (NLC) between UD parameters, we calculated NLC coefficients using Mutual Information (MI) in the scikit–learn Python module (Pedregosa et al., 2011). The MI routine provides both linear and NLC information and it takes on values from zero to infinity. The calculation procedure is based on Shannon entropy (Shannon, 1948) and a generalized formula (Equation 1) in the range of [0, 1] was used to find the correlation coefficients (Linfoot, 1957; Joe, 1989; Vu, Mishra, and Konapala, 2018):

$$\mathrm{NLCC} = \sqrt{[1 - \exp(-2MI)]}, \tag{1}$$

where the NLCC is a nonlinear correlation coefficient normalized between 0 and 1. Note that the NLCC does not show the direction of the relationship (Linfoot, 1957; Numata and Ebenhöh, 2008; Joe, 1989; Laarne et al., 2022). The NLC and linear approaches have been compared in detail by Numata and Ebenhöh (2008), who applied linear (Pearson) and NLC tools to datasets with different distributions and reported that the NLC performed better. Other studies arrived at similar conclusions and further showed that the measurement performance of the NLC method is more advantageous than that of the linear correlation (e.g., Laarne et al., 2022; Rainio, 2022). Moreover, when data are symmetric, linear correlation co-

efficients are not sufficient to determine the relationship between parameters and it is noted that the performance of the NLC approach improves as the noise level increases (Khan et al., 2006; Numata and Ebenhöh, 2008; Vu, Mishra, and Konapala, 2018). The errors of NLCCs were calculated using the Monte Carlo method, which is designed to obtain approximate results for real-world problems using statistical methods (Hahn and Shapiro, 1967; Lowry, 1970). Monte Carlo simulation is an important tool in calculating statistical errors and it is used to calculate the deviation of actual results (see Anderson, 1976, for detail). It can be also used for calculations of errors of NLC coefficients (Alper and Gelb, 1990), since it provides an error estimation for the NLCC at the selected confidence level (here, we choose the confidence level of 0.95) by randomly permuting two parameters and recalculating MI and NLCC values each time.

All sunspots were analyzed using the routine described above and the number of UDs in each sunspot, length of the dataset, umbral area, mean UD parameters, their mean, maximum, and minimum values are listed in Table 2. The number of detected UDs per umbra varies between 481 and 6882 depending on the sunspot. The physical properties of UDs can be summarized as follows: the highest total intensity was found to be 182.93, and the lowest 1.21; maximum/minimum diameters are 246.5/92.2 km; the highest eccentricity is 0.65, while the lowest one is 0.02; the longest lifetime is 120.00 min and the shortest one is 0.75 min; and, lastly, the highest dynamic velocity is 3.80 $\mathrm{km\,s^{-1}}$, while the lowest one is 0.01 $\mathrm{km\,s^{-1}}$.

Data in Table 2 also show that the number of detected UDs is correlated with the umbral area ($r = 0.91$) and is only weakly correlated with the duration of observations ($r = 0.56$). The max, min, and mean values of all parameters are quite close to each other for all sunspot umbras, except the dynamic velocity in NOAA AR 12902. UDs in this AR move much faster as compared to the other ARs. Also, the average lifetime is shorter compared to the other ARs. We will investigate possible reasons for this behavior in detail in a future study.

The correlation analysis produced the following results (see Table 3). The green colors in Table 3(a) and (b) show the meaningful correlation coefficients, while the red colors show not meaningful ones. The green colors in the panel (c) show that the differences between linear and nonlinear correlation coefficients are meaningful, while the red colors show not meaningful differences. The intensity–diameter and diameter–eccentricity pairs show the highest linear and NLC coefficients, while the diameter–lifetime and eccentricity–dynamic velocity pairs showed the lowest linear correlation and eccentricity–lifetime and eccentricity–dynamic velocity pairs showed the lowest NLC coefficients. The NLC coefficients are higher than the linear correlation coefficients without exception. In the case of the diameter–eccentricity pair the linear and NLC coefficients are very close to each other, suggesting that the diameter and eccentricity have a linear relationship, contrary to all other parameters. These results suggest that the dependence of UD parameters may not follow a linear approximation and the NLC method is more suitable for analysis of UD properties.

Figure 6 shows the relationship between the mean UD parameters obtained from each umbra and their total umbral area. The mean diameter, intensity, and eccentricity are exponentially decreasing with the increase of the umbral area, while the mean UD lifetime and dynamic velocity do not depend on the umbral area.

2.4. Temporal Variations of UD Parameters

To visualize the evolution of UD properties we selected several long-living UDs belonging to different ARs and located near the center of an umbra, and plotted their parameters as a function of time (Figure 7).

Table 2 Averaged physical parameters of UDs observed in all sunspot umbras.

Spot no	Dataset	Number of UDs	Umbral area (Mm^2)	Dataset length (min)		Intensity	Diameter (km)	Eccentricity	Lifetime (min)	Dynamic velocity ($km\,s^{-1}$)
1	AR12384	2785	56.66	103.5	Mean	22.69	184.5	0.28	8.12	0.60
					Max	182.93	246.5	0.59	79.75	1.25
					Min	1.26	92.1	0.04	0.75	0.03
2	AR12411	481	33.44	23	Mean	36.60	187.1	0.28	6.24	0.74
					Max	172.91	232.0	0.61	23.00	1.57
					Min	2.81	106.8	0.05	0.75	0.12
3	AR12565 Large Umbra	6882	132.23	149.5	Mean	15.42	185.4	0.28	8.17	0.55
					Max	110.98	244.2	0.58	120.00	1.22
					Min	1.40	98.0	0.03	0.75	0.02
4	AR12565 Small Umbra	1201	24.11	149.5	Mean	19.37	187.2	0.29	9.83	0.46
					Max	140.34	236.9	0.60	83.50	0.99
					Min	1.98	110.5	0.04	0.75	0.01
5	AR12767	2847	62.50	115.5	Mean	26.24	184.6	0.28	9.21	0.52
					Max	134.33	243.2	0.59	102.25	1.10
					Min	1.88	101.7	0.02	0.75	0.02
6	AR12770 Large Umbra	1167	27.92	95	Mean	24.60	189.8	0.31	7.92	0.58
					Max	147.13	238.9	0.56	84.75	1.29
					Min	1.21	102.7	0.04	0.75	0.03
7	AR12770 Small Umbra	641	13.52	95	Mean	35.34	195.4	0.32	8.70	0.48
					Max	139.55	238.5	0.61	81.75	1.10
					Min	1.89	104.7	0.03	0.75	0.02
8	AR12776	2291	58.43	74.25	Mean	24.42	189.0	0.29	6.34	0.85
					Max	163.26	240.4	0.63	63.00	1.91
					Min	1.59	99.6	0.02	0.75	0.04
9	AR12902	2139	26.10	100	Mean	28.09	193.3	0.30	4.05	1.64
					Max	144.43	233.1	0.59	49.25	3.80
					Min	1.44	93.0	0.05	0.75	0.07
10	AR12934	2127	80.01	58.25	Mean	24.34	184.2	0.28	7.78	0.62
					Max	131.88	241.7	0.59	58.25	1.33
					Min	1.66	96.9	0.04	0.75	0.03
11	AR13046	1273	29.59	67.5	Mean	26.93	188.7	0.30	6.14	0.60
					Max	122.14	239.0	0.58	55.50	1.28
					Min	1.37	97.9	0.04	0.75	0.04
12	AR13053	1838	38.80	83.5	Mean	28.02	183.9	0.28	6.96	0.60
					Max	152.56	240.9	0.65	64.75	1.25
					Min	1.85	96.4	0.04	0.75	0.04

Table 3 Linear (a), nonlinear (b) correlation coefficients calculated for mean UD parameters. The bottom panel (c) shows the differences between linear and nonlinear correlation coefficients. The last columns show mean values obtained from 12 ARs.

(a)

	Intensity												
	1	2	3	4	5	6	7	8	9	10	11	12	Mean
Diameter	0.46 ± 0.03	0.30 ± 0.08	0.65 ± 0.01	0.59 ± 0.04	0.59 ± 0.02	0.70 ± 0.03	0.65 ± 0.05	0.67 ± 0.02	0.79 ± 0.02	0.62 ± 0.03	0.64 ± 0.03	0.50 ± 0.04	0.60 ± 0.03
Eccentricity	0.07 ± 0.04	0.18 ± 0.09	0.35 ± 0.02	0.22 ± 0.05	0.06 ± 0.04	0.33 ± 0.05	0.09 ± 0.08	0.21 ± 0.04	0.40 ± 0.04	0.10 ± 0.04	0.16 ± 0.05	0.08 ± 0.05	0.19 ± 0.05
Lifetime	0.29 ± 0.03	0.55 ± 0.07	0.31 ± 0.02	0.28 ± 0.05	0.28 ± 0.03	0.26 ± 0.05	0.25 ± 0.07	0.32 ± 0.04	0.26 ± 0.04	0.33 ± 0.04	0.27 ± 0.05	0.35 ± 0.04	0.31 ± 0.04
Dynamic Velocity	0.09 ± 0.04	0.29 ± 0.08	0.13 ± 0.02	0.13 ± 0.06	0.12 ± 0.04	0.28 ± 0.05	0.14 ± 0.08	0.36 ± 0.04	0.37 ± 0.04	0.19 ± 0.04	0.08 ± 0.05	*0.01 ± 0.05*	0.18 ± 0.05
	Diameter												
Eccentricity	0.49 ± 0.03	0.40 ± 0.08	0.62 ± 0.01	0.62 ± 0.04	0.44 ± 0.03	0.55 ± 0.04	0.54 ± 0.06	0.48 ± 0.03	0.52 ± 0.03	0.45 ± 0.03	0.47 ± 0.04	0.52 ± 0.03	0.51 ± 0.04
Lifetime	0.11 ± 0.04	0.16 ± 0.09	*0.02 ± 0.02*	*0.04 ± 0.06*	0.05 ± 0.04	*0.02 ± 0.06*	0.13 ± 0.08	*0.00 ± 0.04*	*0.03 ± 0.04*	*0.01 ± 0.04*	0.07 ± 0.05	0.09 ± 0.05	0.06 ± 0.05
Dynamic Velocity	*0.03 ± 0.04*	0.24 ± 0.09	0.04 ± 0.02	0.07 ± 0.06	0.05 ± 0.04	0.13 ± 0.06	0.16 ± 0.08	0.12 ± 0.04	0.17 ± 0.04	*0.03 ± 0.04*	*0.05 ± 0.05*	0.07 ± 0.05	0.10 ± 0.05
	Eccentricity												
Lifetime	0.16 ± 0.04	0.30 ± 0.08	0.09 ± 0.02	0.12 ± 0.06	0.15 ± 0.04	0.12 ± 0.06	0.17 ± 0.08	0.12 ± 0.04	0.17 ± 0.04	0.14 ± 0.04	0.18 ± 0.05	0.18 ± 0.04	0.16 ± 0.05
Dynamic Velocity	*0.00 ± 0.04*	0.20 ± 0.09	*0.02 ± 0.02*	*0.06 ± 0.06*	0.06 ± 0.04	0.16 ± 0.06	*0.08 ± 0.08*	0.07 ± 0.04	0.09 ± 0.04	*0.02 ± 0.04*	0.07 ± 0.05	*0.04 ± 0.05*	0.07 ± 0.05
	Lifetime												
Dynamic Velocity	0.12 ± 0.04	*0.08 ± 0.09*	0.12 ± 0.02	0.14 ± 0.06	0.08 ± 0.04	0.12 ± 0.06	0.20 ± 0.08	*0.01 ± 0.04*	0.07 ± 0.04	*0.01 ± 0.04*	0.19 ± 0.05	0.12 ± 0.05	0.10 ± 0.05

(b)

	Intensity												
Diameter	0.57 ± 0.07	0.53 ± 0.10	0.75 ± 0.06	0.75 ± 0.08	0.67 ± 0.07	0.77 ± 0.08	0.71 ± 0.10	0.73 ± 0.07	0.83 ± 0.07	0.68 ± 0.07	0.69 ± 0.08	0.55 ± 0.08	0.69 ± 0.08
Eccentricity	0.35 ± 0.07	0.22 ± 0.10	0.57 ± 0.06	0.57 ± 0.08	0.33 ± 0.07	0.63 ± 0.09	0.45 ± 0.10	0.35 ± 0.07	0.57 ± 0.07	0.38 ± 0.07	0.22 ± 0.08	0.31 ± 0.08	0.41 ± 0.08
Lifetime	0.47 ± 0.07	0.57 ± 0.10	0.55 ± 0.06	0.58 ± 0.08	0.49 ± 0.07	0.47 ± 0.08	0.47 ± 0.10	0.54 ± 0.07	0.44 ± 0.07	0.53 ± 0.07	0.42 ± 0.08	0.44 ± 0.08	0.50 ± 0.08
Dynamic Velocity	0.26 ± 0.07	0.36 ± 0.11	0.36 ± 0.06	0.35 ± 0.08	0.25 ± 0.07	0.47 ± 0.08	0.37 ± 0.10	0.47 ± 0.07	0.43 ± 0.07	0.19 ± 0.07	0.26 ± 0.08	0.33 ± 0.08	0.34 ± 0.08
	Diameter												
Eccentricity	0.50 ± 0.07	0.44 ± 0.10	0.67 ± 0.06	0.66 ± 0.08	0.52 ± 0.07	0.63 ± 0.08	0.57 ± 0.10	0.57 ± 0.07	0.64 ± 0.07	0.46 ± 0.07	0.49 ± 0.08	0.60 ± 0.08	0.56 ± 0.08
Lifetime	0.33 ± 0.07	0.39 ± 0.10	0.28 ± 0.06	0.34 ± 0.08	0.36 ± 0.07	0.48 ± 0.09	0.35 ± 0.10	0.35 ± 0.07	0.33 ± 0.07	0.29 ± 0.07	0.35 ± 0.08	0.40 ± 0.08	0.35 ± 0.08
Dynamic Velocity	0.35 ± 0.07	0.27 ± 0.10	0.38 ± 0.06	0.41 ± 0.08	0.31 ± 0.07	0.52 ± 0.08	0.37 ± 0.10	0.29 ± 0.07	0.35 ± 0.07	0.36 ± 0.07	0.39 ± 0.08	0.38 ± 0.08	0.37 ± 0.08
	Eccentricity												
Lifetime	0.33 ± 0.07	0.39 ± 0.10	0.26 ± 0.06	0.36 ± 0.08	0.32 ± 0.07	0.35 ± 0.08	0.31 ± 0.10	0.34 ± 0.07	0.22 ± 0.07	0.31 ± 0.07	0.33 ± 0.08	0.29 ± 0.08	0.32 ± 0.08
Dynamic Velocity	0.35 ± 0.07	0.36 ± 0.10	0.32 ± 0.06	0.35 ± 0.08	0.33 ± 0.07	0.37 ± 0.08	0.35 ± 0.10	0.32 ± 0.07	0.36 ± 0.08	0.35 ± 0.07	0.32 ± 0.08	0.20 ± 0.08	0.33 ± 0.08
	Lifetime												
Dynamic Velocity	0.45 ± 0.07	0.36 ± 0.10	0.38 ± 0.06	0.41 ± 0.08	0.40 ± 0.07	0.41 ± 0.08	0.51 ± 0.10	0.36 ± 0.07	0.47 ± 0.07	0.32 ± 0.07	0.41 ± 0.08	0.45 ± 0.08	0.41 ± 0.08

(c)

	Intensity												
Diameter	0.11 ± 0.07	0.23 ± 0.10	0.10 ± 0.06	0.16 ± 0.08	0.08 ± 0.07	*0.07 ± 0.08*	*0.06 ± 0.10*	*0.06 ± 0.07*	*0.04 ± 0.07*	*0.06 ± 0.07*	*0.05 ± 0.08*	*0.05 ± 0.08*	0.09 ± 0.08
Eccentricity	0.28 ± 0.07	*0.04 ± 0.10*	0.22 ± 0.06	0.35 ± 0.08	0.27 ± 0.07	0.30 ± 0.09	0.36 ± 0.10	0.14 ± 0.07	0.17 ± 0.07	0.28 ± 0.07	*0.06 ± 0.08*	0.23 ± 0.08	0.22 ± 0.08
Lifetime	0.18 ± 0.07	*0.02 ± 0.10*	0.24 ± 0.06	0.30 ± 0.08	0.21 ± 0.07	0.21 ± 0.08	0.22 ± 0.10	0.22 ± 0.07	0.18 ± 0.07	0.20 ± 0.07	0.15 ± 0.08	0.09 ± 0.08	0.18 ± 0.08
Dynamic Velocity	0.17 ± 0.07	*0.07 ± 0.11*	0.23 ± 0.06	0.22 ± 0.08	0.13 ± 0.07	0.19 ± 0.08	0.23 ± 0.10	0.11 ± 0.07	*0.06 ± 0.07*	*0.00 ± 0.07*	0.18 ± 0.08	0.32 ± 0.08	0.16 ± 0.08
	Diameter												
Eccentricity	*0.01 ± 0.07*	*0.04 ± 0.10*	*0.05 ± 0.06*	*0.04 ± 0.08*	0.08 ± 0.07	*0.08 ± 0.08*	*0.03 ± 0.10*	0.09 ± 0.07	0.12 ± 0.07	*0.01 ± 0.07*	*0.02 ± 0.08*	*0.08 ± 0.08*	0.05 ± 0.08
Lifetime	0.22 ± 0.07	0.23 ± 0.10	0.26 ± 0.06	0.30 ± 0.08	0.31 ± 0.07	0.46 ± 0.09	0.22 ± 0.10	0.35 ± 0.07	0.30 ± 0.07	0.28 ± 0.07	0.28 ± 0.08	0.31 ± 0.08	0.29 ± 0.08
Dynamic Velocity	0.32 ± 0.07	*0.03 ± 0.10*	0.34 ± 0.06	0.34 ± 0.08	0.26 ± 0.07	0.39 ± 0.08	0.21 ± 0.10	0.17 ± 0.07	0.18 ± 0.07	0.33 ± 0.07	0.34 ± 0.08	0.31 ± 0.08	0.27 ± 0.08
	Eccentricity												
Lifetime	0.17 ± 0.07	*0.09 ± 0.10*	0.17 ± 0.06	0.24 ± 0.08	0.17 ± 0.07	0.23 ± 0.08	0.14 ± 0.10	0.22 ± 0.07	*0.05 ± 0.07*	0.17 ± 0.07	0.15 ± 0.08	0.11 ± 0.08	0.16 ± 0.08
Dynamic Velocity	0.35 ± 0.07	0.16 ± 0.10	0.30 ± 0.06	0.29 ± 0.08	0.27 ± 0.07	0.21 ± 0.08	0.27 ± 0.10	0.25 ± 0.07	0.27 ± 0.08	0.33 ± 0.07	0.25 ± 0.08	0.16 ± 0.08	0.26 ± 0.08
	Lifetime												
Dynamic Velocity	0.33 ± 0.07	0.28 ± 0.10	0.26 ± 0.06	0.27 ± 0.08	0.32 ± 0.07	0.29 ± 0.08	0.31 ± 0.10	0.35 ± 0.07	0.40 ± 0.07	0.31 ± 0.07	0.22 ± 0.08	0.33 ± 0.08	0.31± 0.08

The profiles display several kinds of variations. In particular, it seems that there is a general tendency for the parameters to decrease toward the middle of the lifetime. Some of the parameters show oscillations with periods below 6 min. At this moment, it is not clear whether these variations are driven by photospheric oscillations or result from the measurement noise, however, this behavior may prove to be useful for studying the internal structure of sunspots and deserves future attention.

3. Summary and Discussion

UDs appear as a result of magnetoconvection inside the sunspot umbra (Parker, 1979; Schüssler and Vögler, 2006; Bharti, Jain, and Jaaffrey, 2007; Bharti, Beeck, and Schüssler, 2010; Löptien et al., 2021, and references therein). It is also known that the magnetoconvection inside the umbra is modulated by the umbral magnetic field. Therefore, to understand the energy transport in the umbra it is necessary to investigate the physical parameters of UDs and the relationships between these parameters. Yadav, Louis, and Mathew (2018a) provided a very detailed analysis on the relationships between physical properties of UDs and the large-scale properties of sunspots. However, these authors suggested that studies based on higher-resolution data collected for sunspots of various sizes are needed to understand the lack of relationship between the physical properties of UDs and the characteristics

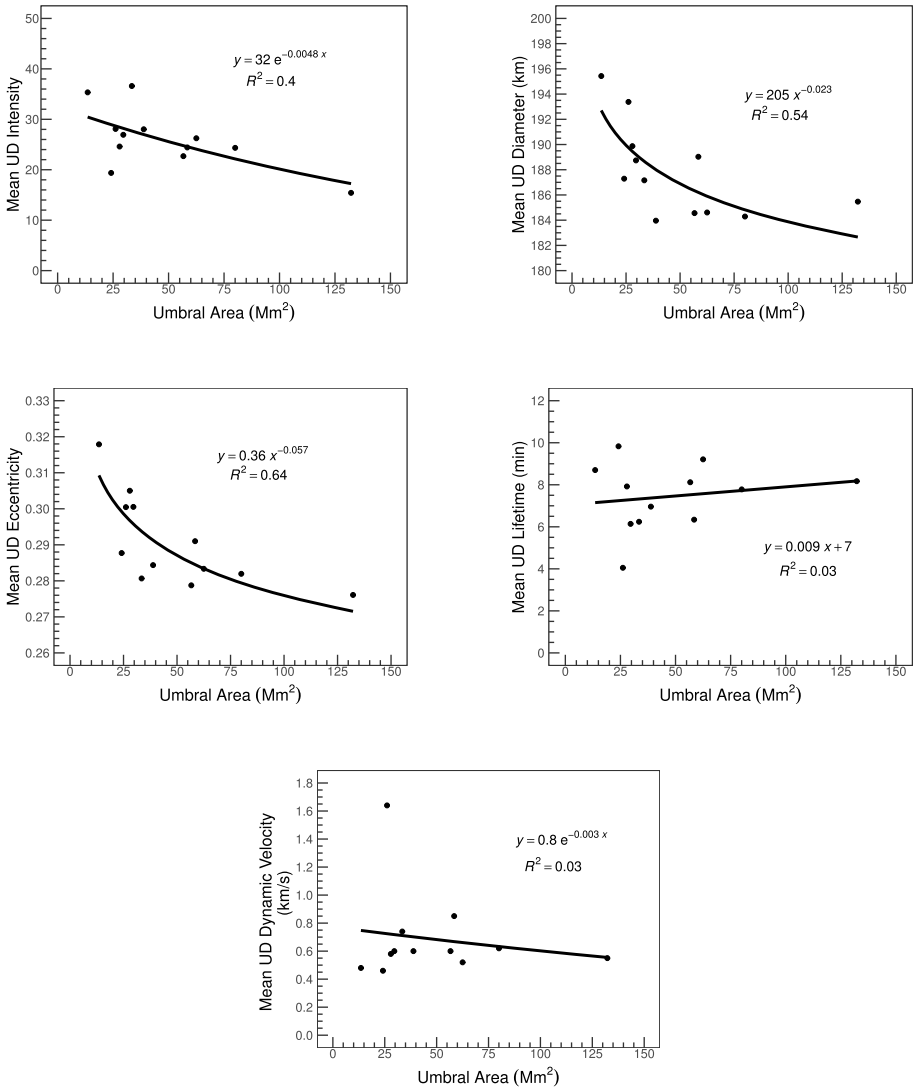

Figure 6 The relationship between umbral areas and mean UD parameters.

of sunspots. Here, we analyzed 12 umbra cores observed in 10 different ARs with the GST broadband imager. The ARs we chose covered the time period from the maximum of Solar Cycle 24 in 2015 until November 2022. We detected a total of 25,672 UDs, and measured their physical parameters. We then utilized both linear and nonlinear correlation analysis methods to investigate the relationships between the UD parameters.

- The range of UD parameters is as follows: the diameter 92.17 – 246.53 km, the eccentricity: 0.02 – 0.65, the lifetime: 0.75 – 120.00 min, and the dynamic velocity: 0.01 – 3.80 km s^{-1}.

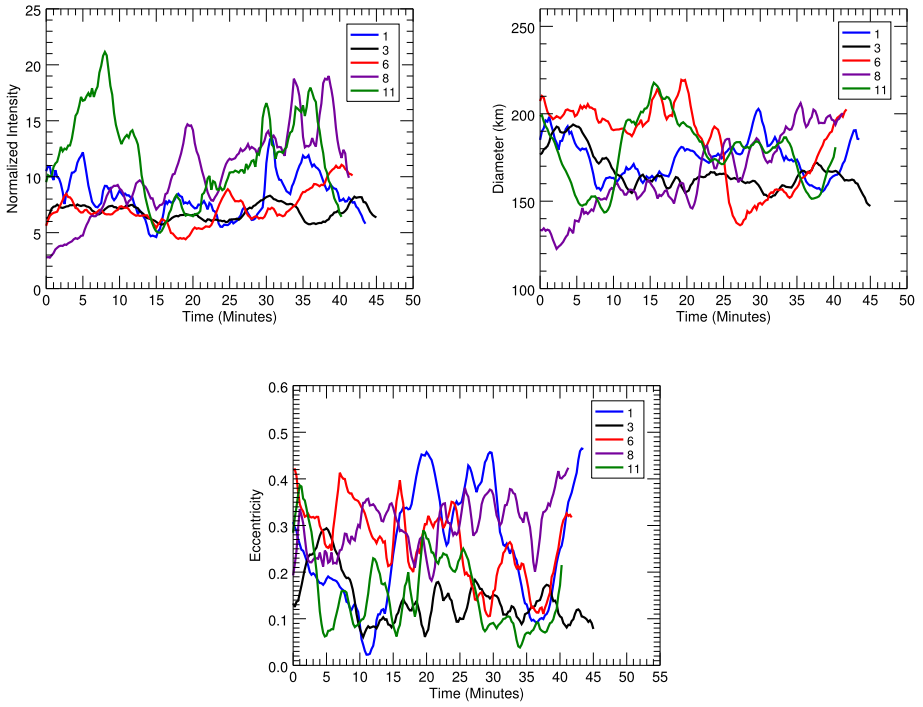

Figure 7 Time profiles of intensity, diameter, and eccentricity plotted for five selected UDs. Note that the temporal variations of all parameters are smoothed with a five-step running average.

- The intensity–diameter and diameter–eccentricity pairs show the highest degree of correlation, while the lowest linear correlation was obtained for the diameter–lifetime and the lowest NL correlation was obtained for the eccentricity–lifetime relationships (see Table 4).
- In general, the NLC coefficients are higher than the linear ones without exception.
- In the case of the diameter–eccentricity relationship, both correlation coefficients are very close to each other.
- The average diameter, intensity, and eccentricity show an exponential decrease with increasing umbral area, while the mean UD lifetime and dynamic velocity do not depend on the umbral area.
- Temporal variations of UD intensity and diameter show different behavior along the UD lifetime and look like they show cyclic behavior.

The lifetimes of UDs have been extensively studied using various datasets and a wide range of values (1 – 65 min) was reported (Watanabe, Kitai, and Ichimoto, 2009; Hamedivafa, 2011; Louis et al., 2012; Feng et al., 2015; Bharti, Beeck, and Schüssler, 2010; Kilcik et al., 2012; Yadav and Mathew, 2018b; Kilcik et al., 2020). In this study, we report the average lifetime of a UD to be 7.6 min and it varies between 0.75 and 120 min. This is nearly twice the previously reported upper limit of the UD lifetime. Approximately 85% of all detected UDs have a lifetime shorter than 15 min. It is likely that the difference is caused by the length of the continuous time series that we used since some of the datasets are longer than 120 min. Note that the lower limit of the UD lifetime (0.75 min) is determined by the

Table 4 Summary of the derived correlations between various UD parameters.

	Diameter	Intensity	Velocity	Lifetime	Eccentricty
Diameter		Yes / No	Yes	Yes / No	Yes
Intensity			Yes / No	Yes / No	Yes
Velocity				No	Yes

applied UD selection criteria. Thus, we may speculate that the lower limit of the UD lifetime could be less than 0.75 min.

It has been reported in previous studies that the diameter of UDs varies between 50 to 750 kilometers (Sobotka and Hanslmeier, 2005; Riethmüller et al., 2008; Watanabe et al., 2012; Kilcik et al., 2012; Feng et al., 2015; Yadav, Louis, and Mathew, 2018a; Kilcik et al., 2020; Ji et al., 2016). Furthermore, Yadav and Mathew (2018b) stated that UDs with a diameter smaller than the resolution limit (0.21″) of the Hinode telescope may exist, but higher-resolution observations are needed to resolve them. In this study, we found that the mean diameters of UDs, determined using 0.1″ resolution data, varied between 92.17 and 246.53 km. These findings confirm previous studies and further refine the lower limit of the UD diameter.

Schüssler and Vögler (2006) found that simulated UDs have horizontally elongated shapes. Kilcik et al. (2012) concluded that all observed UDs without exception have an elongated shape, which can be quantified using an eccentricity parameter, with the mean eccentricity of 0.29 – 0.75 (Kilcik et al., 2012; Feng et al., 2015; Kilcik et al., 2020). Here, we report that the eccentricities of detected UDs vary in the range of 0.02 – 0.65 with a mean value of 0.29.

To describe the velocity of UDs more accurately, Kilcik et al. (2020) introduced the dynamic velocity that measures the UD velocity by taking into account the length of the path traveled by a UD rather than the total displacement. They reported the average dynamic velocity of 0.76 km s^{-1}, with the highest value being 3.84 km s^{-1}. These values are almost twice the numbers reported by Watanabe, Kitai, and Ichimoto (2009) and Feng et al. (2015). In this study, the average dynamic velocity was found to be 0.68 km s^{-1} with the highest velocity reaching 3.80 km s^{-1}. The highest dynamic and average velocity were measured for a large pore in NOAA AR 12902. In comparison to fully developed sunspots, solar pores have weaker magnetic fields and thus convective motions there are less suppressed, which may explain the higher dynamic velocity measured there.

Although the relationships between various UD parameters have been extensively studied, there seems to be no agreement as to what the degree of their correlations are. In Table 4 we summarize all known reports on the correlation between UD parameters. The "yes/no" cells indicate that various authors reached contradicting conclusions. It has been reported in some studies (Bharti, Beeck, and Schüssler, 2010; Ji et al., 2016; Yadav and Mathew, 2018b; Deng, 2019; Kilcik et al., 2020), that larger UDs are brighter and have longer lifetime, while no relationship was found in other studies (Kilcik et al., 2012; Hashem, 2020). Kilcik et al. (2020) reported that the diameter and velocity exhibit a strong relationship. Also, UD intensity was found to be correlated with lifetime (Ji et al., 2016; Deng, 2019; Yadav and Mathew, 2018b), while Hashem (2020) did not find this correlation. Kilcik et al. (2020) reported that UD brightness and dynamic velocity are well correlated, while Deng (2019) noted that the intensity and velocities do not correlate or show a negative correlation. Finally, Kilcik et al. (2020) found no significant relationship between lifetime and dynamic velocity.

Connections between the UD eccentricity and other parameters have not been extensively investigated as of now. Kilcik et al. (2020), found that eccentricities show a weak inverse relationship with the size and the intensity. Later, Kilcik et al. (2020) reported that the UD diameter exhibits a much higher correlation with eccentricity. In this study, a high correlation was observed between diameter and eccentricity, while a low correlation was found between eccentricity and dynamic velocity.

We note that one possible reason for these discrepancies may be due to differences in spatial resolution of the data as well as methods of measurements. In general, we found that the linear and NL correlation coefficients are very close to each other in the case of the diameter–eccentricity relationship. On the other hand, we found that intensity–velocity, intensity–diameter, diameter–lifetime, and diameter–velocity relationships show higher correlation when the NLC approach is used. However, it is not clear at this moment when the nonlinearity appears due to measurement errors or if there is a physical reason for this type of relationship.

Hamedivafa and Sobotka (2004) investigated the temporal variation of UD brightness and area when Joule heating (JH) is present. They found the effect of the JH mechanism is characterized by a specific shape of the temporal variations of UD brightness and area that the brightness of a UD increases simultaneously with the decrease of its area during some time at the end of its lifetime. They assumed this behavior to be a sign of JH phenomena. Watanabe et al. (2012) studied the temporal evolution of UD lifetimes longer than 620 s. They reported that the evolution of central and peripheral UDs, the peak brightness, the brightness ratio, and the diameter show symmetric increase and decrease over time. They found that central and peripheral UDs show mound-shaped temporal evolutionary curves. Hamedivafa (2011), studied the statistical properties of area and brightness of umbral dots using an image-segmentation method and feature-tracking algorithm for the temporal variations of some physical parameters of umbral dots. The author suggested that these variations may not be physical processes in an umbra and are correlated to the image quality (seeing variations). Here, we found different temporal behavior for each umbral dot selected from different ARs. Thus, we may speculate that the different behavior of UD temporal variation may be due to the properties of the umbra to which the UD belongs.

Finally, we found that UDs move on average almost twice as fast as was reported earlier (Watanabe, Kitai, and Ichimoto, 2009; Feng et al., 2015), while their size and lifetime become smaller with increasing spatial and temporal resolution of the data.

Acknowledgments We gratefully acknowledge the use of data from the Goode Solar Telescope (GST) of the Big Bear Solar Observatory (BBSO).

Author contributions M. Ali CALISIR is master and H. Tayfun YAZICI is undergraduate student. Ali KILCIK is their supervisor. These students learned and then did some of the analysis. M. Ali CALISIR mainly focused on image data analysis and H. Tayfun YAZICI did some statistical analysis within the scope of the manuscript. Ali KILCIK taught the methodology to the students and coordinated all study. V. Yurchyshyn prepared all BBSO/GST data sets for the analysis and also contributed during the last step of the manuscript preperation.

Funding BBSO operation is supported by US NSF AGS 2309939 and 1821294 grants and the New Jersey Institute of Technology. The GST operation is partly supported by the Korea Astronomy and Space Science Institute and the Seoul National University. This work, which is part of the MS thesis of M.A. Calisir, was supported by Project 122F004 awarded by the Scientific and Technological Research Council of Turkey. V.Y. acknowledges support from NASA 80NSSC20K0025, 80NSSC20K1282, and 80NSSC21K1671 grants, and NSF AGS 2309939, 2300341, and AST 2108235, 2114201 grants.

Declarations

Competing interests The authors declare no competing interests.

References

Abramenko, V., Yurchyshyn, V., Goode, P., Kilcik, A.: 2010, Statistical distribution of size and lifetime of bright points observed with the New Solar Telescope. *Astrophys. J. Lett.* **725**, L101. DOI.

Alper, J.S., Gelb, R.I.: 1990, Standard errors and confidence intervals in nonlinear regression: comparison of Monte Carlo and parametric statistics. *J. Phys. Chem.* **94**, 4747. DOI.

Anderson, G.: 1976, Error propagation by the Monte Carlo method in geochemical calculations. *Geochim. Cosmochim. Acta* **40**, 1533. DOI.

Berdyugina, S., Solanki, S.K., Frutiger, C.: 2003, The molecular Zeeman effect and diagnostics of solar and stellar magnetic fields – II. Synthetic Stokes profiles in the Zeeman regime. *Astron. Astrophys.* **412**, 513. DOI.

Bharti, L., Beeck, B., Schüssler, M.: 2010, Properties of simulated sunspot umbral dots. *Astron. Astrophys.* **510**, A12. DOI.

Bharti, L., Jain, R., Jaaffrey, S.: 2007, Evidence for magnetoconvection in sunspot umbral dots. *Astrophys. J.* **665**, L79. DOI.

Choudhuri, A.R.: 1986, The dynamics of magnetically trapped fluids. I. Implications for umbral dots and penumbral grains. *Astrophys. J.* **302**, 809. DOI.

Crocker, J., Hoffman, B.: 2007, Cell mechanics. In: Wang, Y.L., Discher, D. (eds.) *Methods in Cell Biology* **83**, Elsevier Academic Press, San Diego, 141. DOI.

Crocker, J.C., Weeks, E.R.: 2021, Particle tracking using IDL. https://physics.emory.edu/faculty/weeks/idl/index.html. Accessed: 2023-06-14.

Danielson, R.E.: 1964, The structure of sunspot umbras. I. Observations. *Astrophys. J.* **139**, 45. DOI. ADS.

Dekking, F.M., Kraaikamp, C., Lopuhaä, H.P., Meester, L.E.: 2005, *A Modern Introduction to Probability and Statistics: Understanding Why and How* **488**, Springer, Berlin. DOI.

Deng, L.: 2019, New Vacuum Solar Telescope observations of solar fine-scale magnetic structures in the lower atmosphere. In: *Solar Polariation Workshop 8* **526**, 229.

Ebadi, H., Abbasvand, V., Pourjavadi, H.: 2017, The study of umbral dots in sunspots based on SOT/Hinode observations. *Astron. Nachr.* **338**, 662. DOI.

Feng, S., Zhao, Y., Yang, Y., Ji, K., Deng, H., Wang, F.: 2015, Identifying and tracking of peripheral and central umbral dots. *Solar Phys.* **290**, 1119. DOI.

Frigge, M., Hoaglin, D.C., Iglewicz, B.: 1989, Some implementations of the boxplot. *Am. Stat.* **43**, 50. DOI.

Hahn, G.J., Shapiro, S.S.: 1967, *Statistical Models in Engineering*.

Hamedivafa, H.: 2011, Kinematics of umbral dots: their typical area, brightness and lifetime. *Solar Phys.* **270**, 75. DOI.

Hamedivafa, H., Sobotka, M.: 2004, Observational evidence of Joule heating in some umbral dots. *Astron. Astrophys.* **428**, 215. DOI.

Hashem, H.: 2020, Comparative study of a sunspot at two different instances of time. *Solar Phys.* **295**, 60. DOI.

Hyndman, R.J., Fan, Y.: 1996, Sample quantiles in statistical packages. *Am. Stat.* **50**, 361. DOI.

Ji, K., Jiang, X., Feng, S., Yang, Y., Deng, H., Wang, F.: 2016, Investigation of umbral dots with the New Vacuum Solar Telescope. *Solar Phys.* **291**, 357. DOI.

Joe, H.: 1989, Relative entropy measures of multivariate dependence. *J. Am. Stat. Assoc.* **84**, 157. DOI.

Khan, S., Ganguly, A.R., Bandyopadhyay, S., Saigal, S., Erickson, D.J. III, Protopopescu, V., Ostrouchov, G.: 2006, Nonlinear statistics reveals stronger ties between ENSO and the tropical hydrological cycle. *Geophys. Res. Lett.* **33**, L24402. DOI.

Kilcik, A., Yurchyshyn, V., Rempel, M., Abramenko, V., Kitai, R., Goode, P., Cao, W., Watanabe, H.: 2012, Properties of umbral dots as measured from the new solar telescope data and MHD simulations. *Astrophys. J.* **745**, 163. DOI.

Kilcik, A., Sarp, V., Yurchyshyn, V., Rozelot, J.-P., Ozguc, A.: 2020, Physical characteristics of umbral dots derived from a high-resolution observations. *Solar Phys.* **295**, 1. DOI.

Laarne, P., Amnell, E., Zaidan, M.A., Mikkonen, S., Nieminen, T.: 2022, Exploring non-linear dependencies in atmospheric data with mutual information. *Atmosphere* **13**, 1046. DOI.

Linfoot, E.H.: 1957, An informational measure of correlation. *Inf. Control* **1**, 85. DOI.

Löptien, B., Lagg, A., van Noort, M., Solanki, S.K.: 2021, Similarities of magnetoconvection in the umbra and in the penumbra of sunspots. *Astron. Astrophys.* **655**, A61. DOI.

Louis, R.E., Mathew, S.K., Rubio, L.R.B., Ichimoto, K., Ravindra, B., Bayanna, A.R.: 2012, Properties of umbral dots from stray light corrected Hinode filtergrams. *Astrophys. J.* **752**, 109. DOI.

Lowry, G.G.: 1970, *Markov Chains and Monte Carlo Calculations in Polymer Science*, Dekker, New York.

Mathew, S., Pillet, V.M., Solanki, S., Krivova, N.: 2007, Properties of sunspots in cycle 23 – I. Dependence of brightness on sunspot size and cycle phase. *Astron. Astrophys.* **465**, 291. DOI.

Numata, J., Ebenhöh, O.: 2008, Measuring correlations in metabolomic networks with mutual information. *Genome Inform.* **20**, 112. DOI.
Parker, E.: 1979, Sunspots and the physics of magnetic flux tubes. IX – Umbral dots and longitudinal overstability. *Astrophys. J.* **234**, 333. DOI.
Pedregosa, F., Varoquaux, G., Gramfort, A., Michel, V., Thirion, B., Grisel, O., Blondel, M., Prettenhofer, P., Weiss, R., Dubourg, V., Vanderplas, J., Passos, A., Cournapeau, D., Brucher, M., Perrot, M., Duchesnay, E.: 2011, Scikit-learn: machine learning in Python. *J. Mach. Learn. Res.* **12**, 2825.
Rainio, O.: 2022, Different coefficients for studying dependence. *Sankhya, Ser. B* **84**, 895. DOI.
Riethmüller, T., Solanki, S., Zakharov, V., Gandorfer, A.: 2008, Brightness, distribution, and evolution of sunspot umbral dots. *Astron. Astrophys.* **492**, 233. DOI.
Rousseeuw, P.J., Ruts, I., Tukey, J.W.: 1999, The bagplot: a bivariate boxplot. *Am. Stat.* **53**, 382. DOI.
Schüssler, M., Vögler, A.: 2006, Magnetoconvection in a sunspot umbra. *Astrophys. J.* **641**, L73. DOI.
Shannon, C.E.: 1948, A mathematical theory of communication. *Bell Syst. Tech. J.* **27**, 379. DOI.
Sobotka, M., Hanslmeier, A.: 2005, Photometry of umbral dots. *Astron. Astrophys.* **442**, 323. DOI.
Solanki, S.K.: 2003, Sunspots: an overview. *Astron. Astrophys. Rev.* **11**, 153. DOI.
Thiessen, G.: 1950, The structure of the sunspot-umbra. *Observatory* **70**, 234.
Thomas, J.H., Weiss, N.O.: 2004, Fine structure in sunspots. *Annu. Rev. Astron. Astrophys.* **42**, 517. DOI.
Tritschler, A., Schmidt, W.: 1997, Some properties of sunspot umbral dots. *Astron. Astrophys.* **321**, 643.
Tukey, J.W.: 1970, *Exploratory Data Analysis: Limited Preliminary Edition*, Addison-Wesley, Ann Arbor.
Tukey, J.: 1977, *Exploratory Data Analysis*, Addison-Wesley, Reading. DOI.
Valio, A., Spagiari, E., Marengoni, M., Selhorst, C.L.: 2020, Correlations of sunspot physical characteristics during solar cycle 23. *Solar Phys.* **295**, 120. DOI.
Vu, T.M., Mishra, A.K., Konapala, G.: 2018, Information entropy suggests stronger nonlinear associations between hydro-meteorological variables and ENSO. *Entropy* **20**, 38. DOI.
Watanabe, H., Kitai, R., Ichimoto, K.: 2009, Characteristic dependence of umbral dots on their magnetic structure. *Astrophys. J.* **702**, 1048. DOI.
Watanabe, H., Rubio, L.R.B., De la Cruz Rodríguez, J., van der Voort, L.R.: 2012, Temporal evolution of velocity and magnetic field in and around umbral dots. *Astrophys. J.* **757**, 49. DOI.
Wöger, F., von der Lühe, O.: 2007, Field dependent amplitude calibration of adaptive optics supported solar speckle imaging. *Appl. Opt.* **46**, 8015. DOI.
Yadav, R., Louis, R.E., Mathew, S.K.: 2018a, Investigating the relation between sunspots and umbral dots. *Astrophys. J.* **855**, 8. DOI.
Yadav, R., Mathew, S.K.: 2018b, Physical properties of umbral dots observed in sunspots: a Hinode observation. *Solar Phys.* **293**, 54. DOI.